

MAGNETIC TOPOLOGIES DUE TO TWO BIPOLAR REGIONS

C. BEVERIDGE, E.R. PRIEST and D.S. BROWN

*Mathematical Institute, University of St Andrews, North Haugh, St Andrews,
KY16 9SS, UK*

Abstract.

The Sun's atmosphere contains many diverse phenomena that are dominated by the coronal magnetic field. To understand these phenomena we must determine the structure of the magnetic field, i.e., the magnetic topology. We study here the topological structure of the coronal magnetic field arising from the interaction of two bipolar regions, for which it transpires that four distinct, topologically stable states are possible. A bifurcation diagram is produced, showing how the magnetic configuration can change from one topology to another as the relative orientation and sizes of the bipolar regions are varied. The changes are produced either by a global separator bifurcation, a local double-separator bifurcation, a new, global separatrix bifurcation or a new, global spine bifurcation.

1. Introduction

The magnetic energy in the solar corona is, in general, much stronger than other types of energy. From this it follows that many dynamic phenomena in the solar corona - including, for instance, solar flares and eruptive prominences - are magnetically driven.

The coronal field arises from a large number of magnetic flux sources on the photosphere, which continually move around, merging and cancelling, appearing and disappearing. It is this continuous evolution that produces the enormous complexity of the coronal field structure. Furthermore, many of the dynamic phenomena occur only in complex configurations when topologically distinct parts of the magnetic field are interacting with each other (e.g., in flares, Lau, 1993; Aulanier *et al.*, 1998; Fletcher *et al.*, 2001). An important long-term project, then, is to categorise and study the different types of topology of the coronal magnetic field as a prerequisite for a full understanding of the mechanisms that control these dynamic phenomena.

In this paper, our aim is to focus on the simplest class of complex topologies that occurs in practice in a solar active region, namely the field due to two dipoles. This scenario is of some importance, since it arises reasonably frequently, for instance, when a new bipole emerges into a pre-existing bipolar region,



© 2001 Kluwer Academic Publishers. Printed in the Netherlands.

One way of describing the complexity of a configuration is to calculate the ‘magnetic skeleton’ of the field (Priest, Bungey and Titov, 1997). This consists of the positions of the sources and any null points along with their spine curves and fan separatrix surfaces, as well as any separators.

Nulls are points where the magnetic field vanishes. Their linear structure has been studied in detail by Parnell *et al.* (1996), who find that the field near a null point may in general be written in the form $\mathbf{B} = \mathbf{M} \cdot \mathbf{r}$, where \mathbf{r} is the position vector $(x, y, z)^T$ and \mathbf{M} is the matrix:

$$\mathbf{M} = \begin{bmatrix} 1 & \frac{1}{2}(q - j_{\parallel}) & 0 \\ \frac{1}{2}(q + j_{\parallel}) & p & 0 \\ 0 & j_{\perp} & -(p + 1) \end{bmatrix},$$

where j_{\parallel} and j_{\perp} represent the current parallel and perpendicular (respectively) to the spine, while p and q are potential field parameters.

In view of $\nabla \cdot \mathbf{B} = \mathbf{0}$, the trace of \mathbf{M} - and hence the sum of its eigenvalues - is also zero (see also Cowley, 1973; Lau and Finn, 1991). In the non-degenerate potential case, which is the one we shall consider here, one of the eigenvalues is of the opposite sign to the other two. The eigenvector associated with the first defines a spine field line; the other two define a fan plane (Lau and Finn, 1990). Figure 1 illustrates this structure.

The field lines beginning in this fan plane form a separatrix surface, which splits the space into regions of different connectivity. Where two separatrices intersect, a field line connecting two null points exists. This field line, known as a separator, lies at the boundary of four regions of different connectivity, and is a prime location for reconnection to occur (Figure 2) by so-called ‘separator’ reconnection (Priest and Titov, 1996; Galsgaard and Nordlund, 1996; Longcope, 1996; Galsgaard *et al.*, 2000.) Brown and Priest (1999) give a topological analysis of such separators.

The arrangement of these structures determines their topology. We examine here the topologies due to a small number of discrete point sources in the photosphere, following for instance Gorbachev *et al.* (1988). They gave a preliminary treatment of four sources and found that coronal nulls can exist in such a configuration, and that separators do not occur in every case. They also showed that a null line can exist. Their bifurcation analysis, however, was limited, since they concerned themselves with existence proofs rather than a full quantitative analysis.

Further work on coronal nulls has been carried out by Inverarity and Priest (1999), and Brown and Priest (2001), who consider general solu-

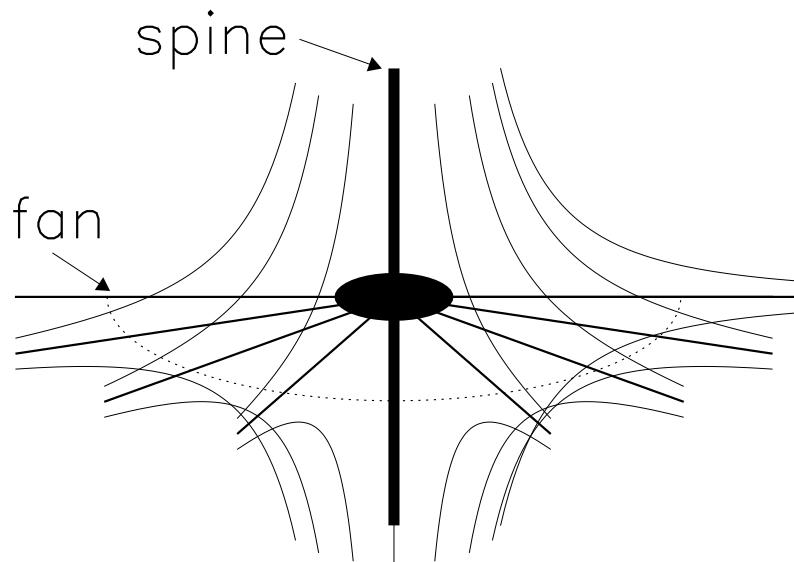


Figure 1. The structure of the magnetic field near a null point (the heavy dot). The spine is represented by a heavy line, the fan plane by medium-weight lines and some field lines by thin curves.

tions for such nulls and how they can bifurcate out of the photosphere into the corona.

This study is similar to work undertaken by Priest, Bungey and Titov (1997) on two-source and simple three-source cases, and by Brown and Priest (1999) who completely classified the three-source scenario. They found that eight topologies are possible in that case and analysed the bifurcations between them.

We will extend their analysis to four sources by considering two dipoles of different strengths. We find just four distinct topologies, some of which have previously been examined in the Gorbachev *et al.* (1988) paper. There are four distinct types of bifurcation between the topologies. Two of them have been found before, namely the ‘local double-separator’ bifurcation (in which a null is created or destroyed) and the ‘global separator’ bifurcation (in which a separator appears or disappears). The other two bifurcations are new, and we refer to them as ‘global separatrix’ and ‘global spine’ bifurcations.

In Section 2, we outline our assumptions and the model we shall be using. Section 3 details the different types of topology that can be created with this model, and Section 4 examines the bifurcations between them. We conclude with a discussion of our results.

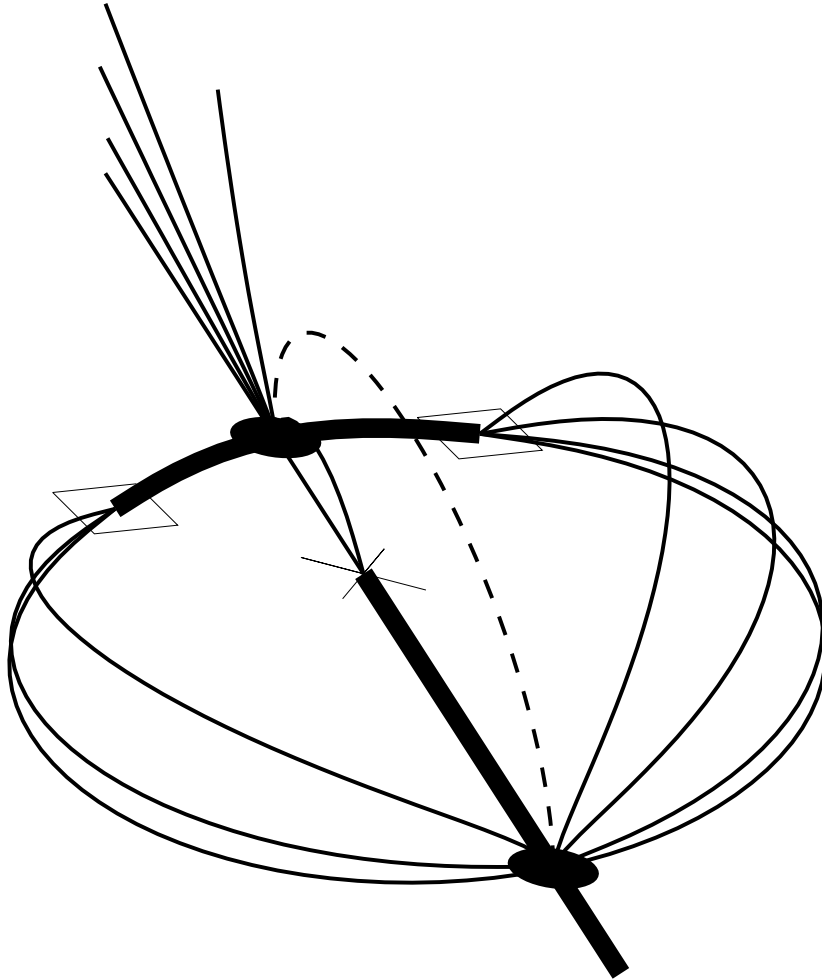


Figure 2. A typical three-source topology - the intersecting case. The crosses and diamonds represent positive and negative sources, respectively; the large dots are null points. The dashed line is a separator, which is the line of intersection of the two separatrix surfaces (containing the lighter solid field lines) which here form a dome and a wall. The thick solid lines are spine field lines.

2. Assumptions and Model

The coronal magnetic field is often considered to be force-free (since $\beta \ll 1$ and motions are much slower than the Alfvén speed). As we are studying the topology of the field, we will make the further assumption that the field is potential for the sake of simplicity. Force-free fields are unlikely to have any different topological states, although the precise parameter values that produce changes between them will certainly depend on how far from potential the field is (Brown and Priest, 2000). This would introduce an extra set of parameters into the already complicated analysis presented here.

We consider two pairs of flux sources (for instance, sunspot pairs) situated in the photosphere, which we model locally as a plane, taking the corona to be the half-space above it. The field at a distance r from a sunspot or other flux source of non-zero radius R does not differ significantly from that of a point source when $r \gg R$. It is reasonable, then, to model the flux sources here as point sources provided we are not too close to them.

For a set of n discrete sources placed at \mathbf{r}_i with strengths ϵ_i ($i = 1 \dots n$), the field is

$$\mathbf{B}(\mathbf{r}) = \sum_{i=1}^n \frac{\epsilon_i(\mathbf{r} - \mathbf{r}_i)}{|\mathbf{r} - \mathbf{r}_i|^3}.$$

We examine the two-dipole case, that is to say, with $n = 4$, $\epsilon_1 = -\epsilon_2$ and $\epsilon_3 = -\epsilon_4$. We can rescale the geometry without loss of generality by choosing two of the source locations as $\mathbf{r}_1 = (1, 0)$, $\mathbf{r}_2 = (-1, 0)$. We can also rescale the source strengths so that $\epsilon_1 = 1$, $\epsilon_2 = -1$, $\epsilon_3 = -\epsilon_4 = \epsilon < 1$ with $0 \leq \epsilon \leq 1$. In other words, by scaling we can reduce the ten dimensional parameters in the initial setup to just five independent dimensionless parameters.

Our expression for $\mathbf{B}(\mathbf{r})$ is then:

$$\mathbf{B}(\mathbf{r}) = \frac{(\mathbf{r} - \hat{\mathbf{x}})}{|\mathbf{r} - \hat{\mathbf{x}}|^3} + \frac{-(\mathbf{r} + \hat{\mathbf{x}})}{|\mathbf{r} + \hat{\mathbf{x}}|^3} + \frac{\epsilon(\mathbf{r} - \mathbf{r}_3)}{|\mathbf{r} - \mathbf{r}_3|^3} + \frac{-\epsilon(\mathbf{r} - \mathbf{r}_4)}{|\mathbf{r} - \mathbf{r}_4|^3}.$$

The five parameters are the value of ϵ and the coordinates of \mathbf{r}_3 and \mathbf{r}_4 in the plane $z = 0$. Since five is still too many parameters to allow a comprehensive study, we here fix ϵ and move the poles of the weaker dipole around a fixed centre (x_0, y_0) , to leave just two parameters, namely the x and y coordinates of the weaker source.

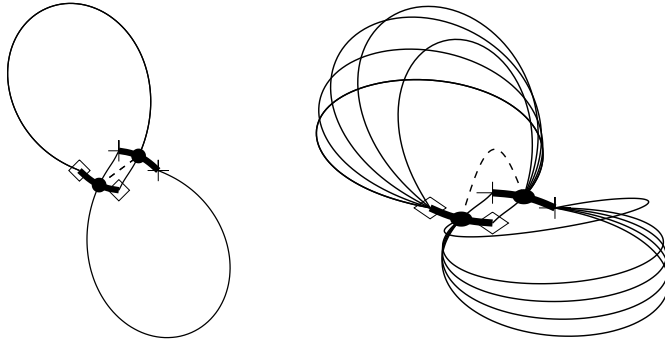


Figure 3. Intersecting state, as seen from above (left) and from the side (right) produced by two sources (crosses) and two sinks (diamonds). The fan of each null (heavy dot) defines a separatrix surface (thin solid lines). In this case the separatrices form domes which intersect in a separator (dashed line.) There are four distinct regions of connectivity.

3. Topologies

An arrangement of four discrete flux sources in the photospheric plane must have two null points in that plane. It is the different possible connectivities of their fan and spine field lines which define the four different topologies of the overlying coronal magnetic configuration, as follows.

3.1. INTERSECTING STATE

If the fan field lines for a null in the plane connect to different sources, and the nulls are of different sign, then we have the intersecting state (Figure 3). The fans of the two nulls here form two separatrix domes which intersect in a separator field line. This state occurs usually when the distance across the weaker bipole is small enough for there to be field lines connecting across it, or so large that the stronger bipole can be considered a point dipole.

3.2. DETACHED AND NESTED STATES

If, instead, all the fan field lines from one null connect to one source and all those in the other fan connect to another, the state is either detached (Figure 4) or nested (Figure 5). The only difference between these two states is that in the nested state one of the separatrix domes envelops the other, while the detached state is topologically identical to two independent and unbalanced pairs of sources. These states generally

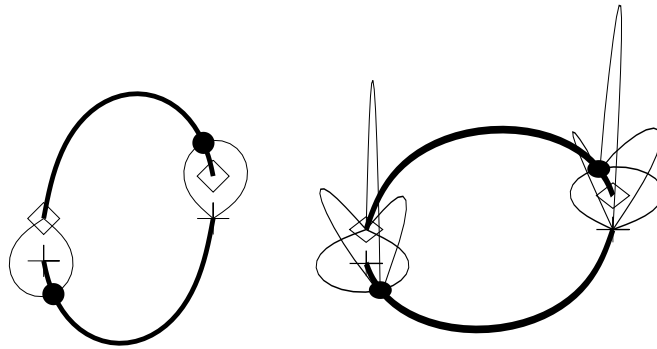


Figure 4. Detached state. The two separatrix domes do not intersect. There is no separator and only three regions of connectivity.

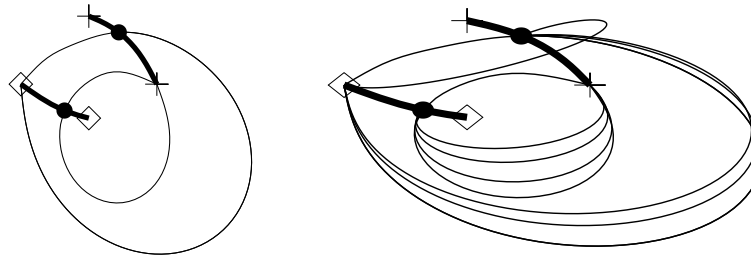


Figure 5. Nested state. One separatrix dome surrounds the other. There are three regions of connectivity and no separator exists. These are schematic plots; in practice both separatrix domes are often much larger and are far from circular.

occur when the distance across the weaker bipole is comparable to that across the stronger while its strength is significantly smaller.

3.3. CORONAL NULL STATE

Finally, if the nulls are of the same sign, a further two nulls of the opposite sign are required to balance them. Because of the symmetry in the plane, one must be above the photosphere (i.e., a coronal null) and the other is below the region $z > 0$ (so we ignore it). This is the coronal null state (Figure 6).

4. Bifurcations

Let us consider the arrangements of the sources that produce the various topological states. The fixed sources of strength ± 1 are located at

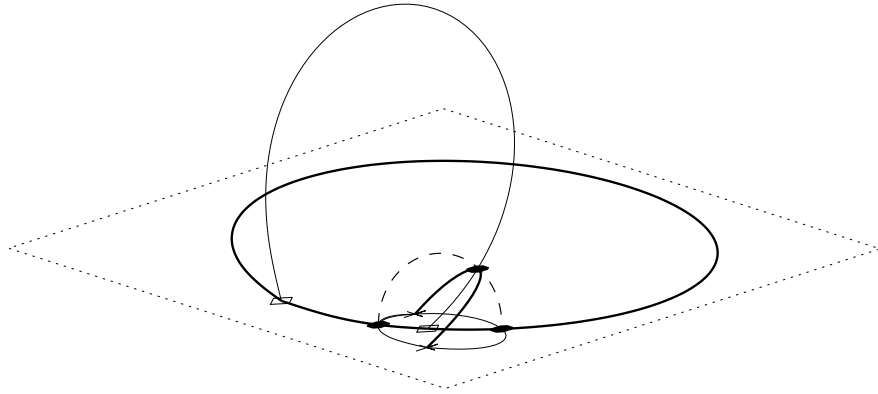


Figure 6. Coronal null state. There are four regions of connectivity and two separators (each of which is a field line joining the coronal null to a null in the photospheric plane.)

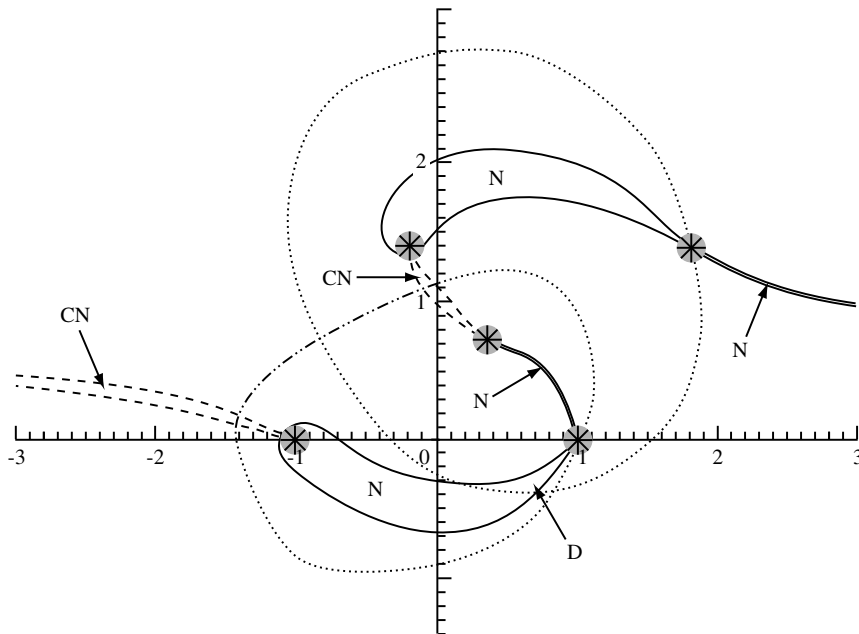


Figure 7. Bifurcation diagram for $\epsilon = 0.8$ and $(x_0, y_0) = (0.4, 0.7)$. The solid lines represent global separator bifurcations; the dashed lines are local double-separator bifurcations. The dotted lines represent the global separatrix bifurcation and the dot-dashed line is a global spine bifurcation. The label CN denotes coronal null regions, D represents the detached regions and N the nested areas. The remaining regions are intersecting states.

$(\pm 1, 0)$, while the centre of the weaker dipole is located at a fixed point $(x_0, y_0) = (0.4, 0.7)$. Figure 7 is a bifurcation diagram which shows the nature of the topology when the positive moving source number 3, with strength $\epsilon = 0.8$ is located at any point (x, y) in the plane $z = 0$. Its corresponding negative source is located at $(2x_0 - x, 2y_0 - y)$.

There are five critical points (marked with stars), where regions of several different topologies meet. These are the rotation centre (x_0, y_0) , the locations of the two fixed sources $(\pm 1, 0)$ and their reflections about the centre $(2x_0 \pm 1, 2y_0)$, where two of the sources merge.

Several regions of different topology are immediately apparent. There are two coronal null regions: one beginning at $(-1, 0)$ and tending towards $(-\infty, y_0)$, the other lying between $(2x_0 - 1, 2y_0)$ and (x_0, y_0) . Nested-type states exist in two crescent areas, one linking $(2x_0 - 1, 2y_0)$ and $(2x_0 + 1, 2y_0)$ and the other joining $(-1, 0)$ and $(1, 0)$. This lower crescent is split into a nested region (extending from the negative fixed source) and a detached region (near the positive source). Between the rotation centre $(0.4, 0.7)$ and $(1, 0)$ is a nested region too narrow to be shown in the figure; likewise between $(2x_0 + 1, 2y_0)$ and (∞, y_0) lies a thin nested region.

4.1. GLOBAL SEPARATOR BIFURCATION

The global separator bifurcation, which creates or destroys a separator, is well understood (Brown and Priest, 1999). It changes the state from intersecting to detached or nested, and vice versa. It is marked in the bifurcation diagram by a solid line. Figure 8 shows an example of the changes in the skeleton, as seen from above, during such a bifurcation from an intersecting to a detached state. On the left there are two separatrix domes intersecting in a separator. As the two domes move apart, the separator falls in height until, at the moment of bifurcation (middle), it reaches the plane and vanishes, to leave the detached topology (right).

4.2. LOCAL DOUBLE-SEPARATOR BIFURCATION

The local double-separator bifurcation, which changes the topology from an intersecting to a coronal null state and vice versa, is also well understood (Brown and Priest, 2001). Figure 9 shows the process by which one of the photospheric nulls splits into three nulls, one of which remains in the photosphere, another rises into the corona and the other disappears beneath the photospheric plane. This bifurcation is denoted in Figure 7 by a dashed line.

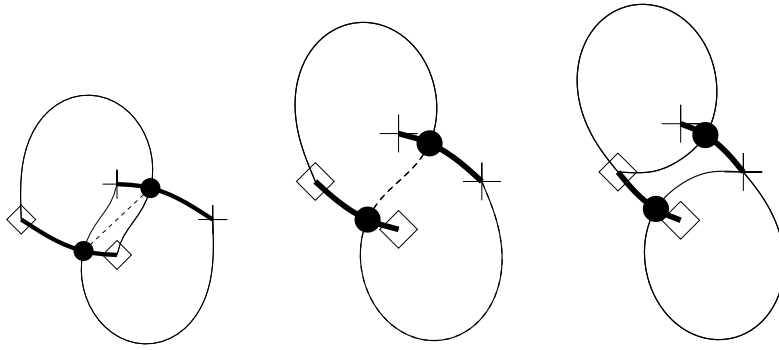


Figure 8. Global separatrix bifurcation from an intersecting state (left) to the detached state (right).

4.3. GLOBAL SEPARATRIX BIFURCATION

It is also possible for one intersecting state to bifurcate into another intersecting state (Figure 10) by way of a new global separatrix bifurcation. A change from a detached to a nested state or vice versa may also take place by a separatrix bifurcation. In both cases, one separatrix grows progressively larger until it becomes a separatrix wall and ‘wraps around’ another, smaller separatrix dome. This is marked by the dotted lines in Figure 7.

4.4. GLOBAL SPINE BIFURCATION

Finally, a new global spine bifurcation (Figure 11) has a similar effect to a global separatrix bifurcation, but here it is the spine rather than the separatrix dome that extends to infinity. It is marked by the dash-double-dot line in Figure 7.

5. Discussion

In reality, the solar surface contains many thousands of flux ‘sources’ in the form of sunspots, ephemeral regions, network elements and intense flux tubes, which are constantly appearing, fragmenting, merging, cancelling and disappearing. The overlying coronal magnetic field has therefore an incredibly complex nature.

However, studying simpler topologies due to three or four sources is important, since these act as building blocks for the whole corona. So far, a complete study of the topology of three sources has been undertaken (Brown and Priest, 1999). An exhaustive study of the topology

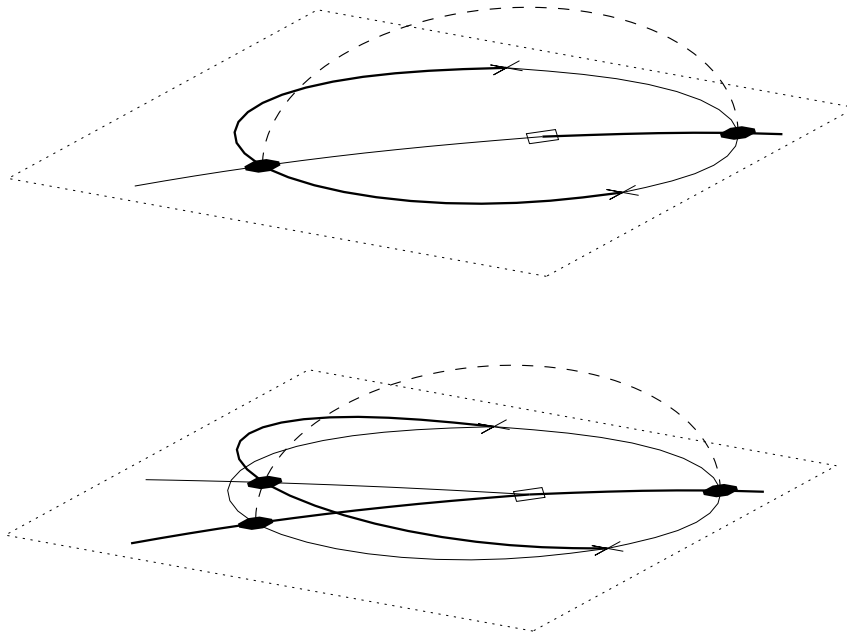


Figure 9. Local double-separator bifurcation. The left-hand null in the left-hand diagram, splits into three nulls, one of which is hidden below the plane.

due to four sources is far more difficult to complete since it contains two more parameters, namely the position coordinates of the fourth source. (If there is an imbalance, a third extra parameter, namely the strength of the imbalance would be included). Until now, only a cursory analysis has been reported of a few special cases with four sources.

Here we focus on the subcase of the set of topologies due to two bipolar regions, which is physically important on the Sun since flux appears by the emergence of bipoles. Also, the interaction of a new bipole with a pre-existing bipole is a very common occurrence.

The resulting bifurcation diagram (Figure 7) is rather complicated and includes four different types of bifurcation (namely, a global separator bifurcation, a local double-separator bifurcation, a global separatrix bifurcation and a global spine bifurcation, the last two of which are new). They allow changes of topology between four distinct states, namely an intersecting state, a detached state, a nested state and a coronal null state. Calculating this bifurcation diagram is made particularly difficult by the appearance of the global spine and global separatrix bifurcations, in which parts of the skeleton move off to infinity and are not easily found by automatic computational algorithms.

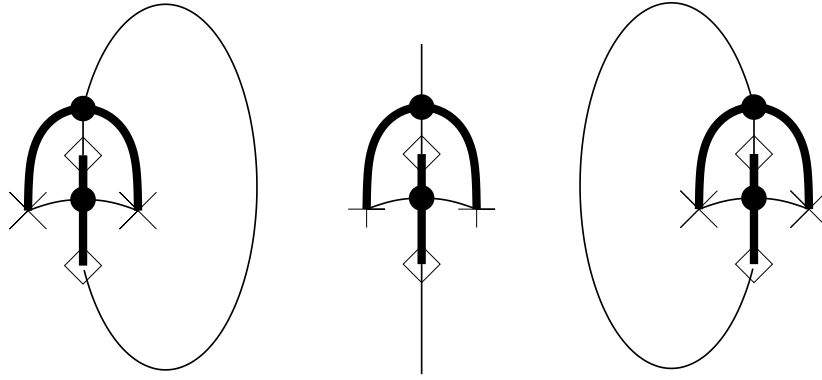


Figure 10. Global separatrix bifurcation (schematic plot). One separatrix dome grows (left), until it becomes a separatrix wall (centre) and wraps around the other dome (right.)

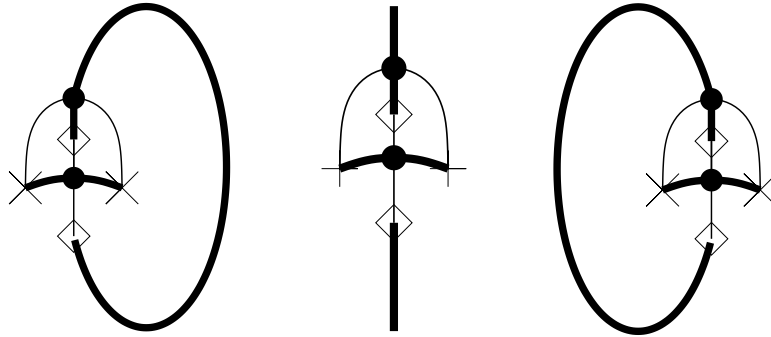


Figure 11. Global spine bifurcation (schematic plot). One spine grows (left), reaches to infinity (centre), and ‘wraps around’ to the other side (right.)

We expect that extending the analysis to force-free fields or changing the values of our fixed parameters - the moving bipole strength and the position of its centre - will change the size and shape of the regions produced, but is unlikely to produce fundamentally different topologies or bifurcations. Although understanding these topologies is an important task in its own right, it will be interesting in the future to undertake numerical MHD experiments on various bifurcations that we have identified in order to determine their dynamical consequences for the Sun’s atmosphere.

Acknowledgements

The authors are grateful for financial support from the UK Particle Physics and Astronomy Research Council and from the EU PLATON network (grant no. HPRN-CT-2000-00153).

References

- Aulanier, G., Démoulin, P., Schmieder, B., Fang, C. and Tang, Y.: 1998, Magneto-hydrostatic model of a bald patch flare, *Solar Physics* **183**, 369-388.
- Brown, D.S. and Priest, E.R.: 1999, Topological bifurcations in 3D magnetic fields, *Proc R Soc London Ser A* **455**, 3931-3951.
- Brown, D.S. and Priest, E.R.: 2000, Topological differences and similarities between force-free and potential models of coronal magnetic fields, *Solar Physics* **194**, 197-204.
- Brown, D.S. and Priest, E.R.: 2001, The topological behaviour of 3D null points in the Sun's corona, *Astron. and Astrophys.* **367**, 339-346.
- Cowley, S.W.H.: 1973, A qualitative study of the reconnection between the Earth's magnetic field and an interplanetary field of arbitrary orientation, *Radio Science* **8**, 903-913.
- Fletcher, L., Metcalf, T.R., Alexander, D., Ryder, L.A., Brown, D.S. and Nightingale, R.W.: 2001, Evidence for the flare trigger site and 3D reconnection in multiwavelength observations of a solar flare, *Ap. J.* **554**, 451-463.
- Galsgaard, K., Parnell, C.E. and Blaizot, J.: 2000, Elementary Heating Events - Magnetic interactions between two flux sources, *Astron. and Astrophys.* **362**, 383-394.
- Galsgaard, K. and Nordlund, Å: 1997, Heating and activity of the solar corona. 3. Dynamics of a low-beta plasma with 3D null points, *J. Geophys. Res* **102**, 231-248.
- Gorbachev, V.S., Kel'ner, S.R., Somov, B.V. and Shverts, A.S.: 1988, A new topological approach to the question of the trigger for solar flares, *Soviet Astron.* **32**, 308-314.
- Inverarity, G. and Priest, E.R.: 1999, Magnetic null points due to multiple sources of solar photospheric flux, *Solar Physics* **186**, 99-121.
- Molodenskii, M.M. and Syrovatskii, S.I.: 1977, Magnetic fields of active regions and their zero points, *Soviet Astron.* **21**, 734-741.
- Lau, Y.T.: 1993, Magnetic nulls and topology in a class of solar flare models, *Solar Physics* **148**, 301-324.
- Lau, Y.T. and Finn, J.M.: 1990, 3D kinematic reconnection in the presence of field nulls and closed field lines, *Ap. J.* **350**, 672-691.
- Lau, Y.T. and Finn, J.M.: 1991, 3D kinematic reconnection in plasmoids, *Ap. J.* **366**, 577-599.
- Longcope, D.W.: 1996, Topology and current ribbons: a model for current reconnection and flaring in a complex evolving corona, *Solar Physics* **169**, 91-121.
- Parnell, C.E., Smith, J.M, Neukirch, T. and Priest, E.R.: 1996, The structure of three-dimensional magnetic neutral points, *Phys. Plasmas* **3**, 759-770.

- Priest, E.R., Bungey, T.N. and Titov, V.S.: 1997, The 3D topology and interaction of complex magnetic flux systems, *Geophysical and Astrophysical Fluid Dynamics* **84**, 127-163.
- Priest, E.R., and Titov, V.S.: 1996, Magnetic reconnection at 3D null points, *Phil. Trans. R. Soc. London, Ser. A* **354**, 2951-2992.